Commun. Comput. Phys.
doi: 10.4208/cicp.120811.200112a

Vol. **12**, No. 5, pp. 1293-1306
November 2012

Parallel Tempering Simulation on Generalized Canonical Ensemble

Shun Xu[1,2,3], Xin Zhou[2,3,*] and Zhong-Can Ou-Yang[4]

[1] *School of Computer Science and Engineering and Guangdong Key Laboratory of Computer Network, South China University of Technology, Guangzhou 510641, China.*
[2] *College of Physical Sciences, Graduate University of Chinese Academy of Sciences, Beijing 100190, China.*
[3] *Asia Pacific Center for Theoretical Physics, Pohang, Gyeongbuk 790784, Korea.*
[4] *Institute of Theoretical Physics, Chinese Academy of Sciences, Beijing 100190, China.*

Received 12 August 2011; Accepted (in revised version) 20 January 2012

Available online 8 May 2012

Abstract. Parallel tempering simulation is widely used in enhanced sampling of systems with complex energy surfaces. We hereby introduce generalized canonical ensemble (GCE) instead of the usual canonical ensemble into the parallel tempering to further improve abilities of the simulation technique. GCE utilizes an adapted weight function to obtain a unimodal energy distribution even in phase-coexisting region and then the parallel tempering on GCE yields the steady swap acceptance rates (SARs) instead of the fluctuated SARs in that on canonical ensemble. With the steady SARs, we can facilitate assign the parameters of the parallel tempering simulation to more efficiently reach equilibrium among different phases. We illustrate the parallel tempering simulation on GCE in the phase-coexisting region of 2-dimensional Potts model, a benchmark system for new simulation method developing. The result indicates that the new parallel tempering method is more efficient to estimate statistical quantities (i.e., to sample the conformational space) than the normal parallel tempering, specially in phase-coexisting regions of larger systems.

PACS: 02.70.Tt, 05.10.Ln, 05.50.+q

Key words: Parallel tempering, generalized canonical ensemble, enhanced sampling, Potts model.

1 Introduction

To overcome the difficulties in sampling thermodynamical systems with the complex energy landscape, parallel tempering (PT, which is also referred to as replica exchange) [1,2]

*Corresponding author. *Email addresses:* alwintsui@gmail.com (S. Xu), xzhou@gucas.ac.cn (X. Zhou), oy@itp.ac.cn (Z.-C. Ou-Yang)

was developed and applied widely in simulations of many different systems. In the standard PT, M identical systems (replicas) with their respective temperature T_i are performed in parallel, two neighboring replicas exchange their microscopic configurations (or temperatures equivalently) with a Metropolis probability. Due to the configuration exchanges among replicas, PT is expected to have stronger abilities than the conventional single-replica simulations in overcoming high free energy barriers which separate different conformational regions. Since the implementation of PT is simple in comparison with some other enhanced sampling methods, PT has been widely applied in simulations of physical and biological systems, by using both Monte Carlo simulation and Molecular Dynamics simulation (see a review [3]).

Efficient PT should have a significant swap acceptance rate (SAR, the average acceptance probability of the configuration exchanges). One of the primary issues of PT is how to pre-set the parameters such as temperatures. For example, in canonical ensemble (fixed number of particle N, volume V and temperature T) parallel tempering (NVT-PT), we need to set the temperature of each replica to make SAR between each two adjacent replicas be significant. Usually one performs a short PT simulation by initially supposing a set of temperatures for the replicas and estimates SARs, then adjusts temperatures of replicas based on the estimated SARs and runs another short PT simulation. Iterating the process to make SARs reach a suitable value, such as $20\sim30\%$ [4]. However, this way does not always work well, specially in phase-coexisting regions [5, 6]. In these regions, conformational trajectories could go back and forth between the different phases, the values of SAR may be large while the adjacent replicas locate in the same phase, but become very small while they locate in different phases. Thus SAR becomes highly time-dependent, it is hard to estimate SAR from short segments of simulations to set temperatures of replicas. In addition, in such cases, it is questionable that the average value of SAR in an entire PT simulation can characterize the efficiency of PT in sampling. For equilibrating different phases, we actually need sufficient inter-phase exchange events rather than total exchange events which measured by the average SAR.

SAR depends on the overlap of conformational energy distributions between adjacent replicas [7]. Considering the fact that the energy fluctuation, σ, is proportional to $N^{1/2}$, where N is the size of system, for completely covering an interesting energy range, ΔE, which is proportional to N, the number of required replicas, $n\sim\Delta E/\sigma\sim N^{1/2}$. The simple estimation implies PT is more efficient in small systems. J. de Pablo and coworkers [8] had quantified this relationship between the overlap of distribution and the value of SAR. They regard the energy distribution of replica as a Gaussian form and SAR of the two adjacent replicas is approximate to

$$P_{acc}\simeq\operatorname{erfc}\Big(\frac{\kappa}{\sqrt{2}}\Big), \tag{1.1}$$

where $\kappa\equiv(\bar{E}_2-\bar{E}_1)/(\sigma_1+\sigma_2)$, $\bar{E}_1$ and $\bar{E}_2$ are the mean energy of two Gaussian distributions and σ_1 and σ_2 are variances, respectively. Other researchers [9–11] have also discussed the relationship between the overlap of distribution and SAR. All of these in-

vestigations are beneficial to estimate the number of required replicas in PT and to set temperatures of replicas.

The Gaussian-like (or unimodal) energy distributions of simulation trajectories usually indicates a single phase and then almost constant SARs in PT, thus we might estimate SAR and set parameters of PT from short trial simulations by the traditional way. However, in phase-coexisting regions, the energy distribution of canonical trajectory is usually a multiple-peak rather than unimodal function. Eq. (1.1), which was derived from the Gaussian-form energy distribution supposition [8], will not give the estimate of SAR. Then the traditional way to set temperatures of replicas is no longer efficient. The difficulties could be overcome by replacing the canonical ensemble with a generalized ensemble to implement PT simulation, if the energy distribution in the generalized ensemble is still unimodal even in phase-coexistence regions. Actually, many known ensembles satisfy the requirement, such as the Gaussian ensemble developed by Hetherington et al. [12, 13], the Ray's micro-canonical ensemble [14]. In this work, we present a generalized canonical ensemble (GCE) to replace the canonical ensemble in traditional PT simulations. GCE is a direct generalization of canonical ensemble. It can be also thought as a derivative of Hetherington's Gaussian ensemble [12,13]. More details about GCE are given in the next section. In one word, the energy distribution in GCE can be unimodal even in phase-coexisting regions, thus we can easily set the parameters of replicas in the GCE-PT method, easily reach equilibrium between different phases and more efficiently detect multiple-phase coexistence.

2 Method and theory

In the section, we first introduce the generalized canonical ensemble (GCE) and derive the condition to form a Gaussian-like energy distribution function in GCE. Then we combine the parallel tempering(PT) with the GCE to form GCE-PT simulation method. Finally, we derive the acceptance criterion of GCE-PT and theoretically analyze the abilities of GCE-PT in sampling and its advantages in comparison with PT on canonical ensembles (NVT-PT).

2.1 Generalized canonical ensemble

Simulation ensembles existing in references [12–18] differs in their conformational distribution functions,

$$W(r) \propto e^{-f(V(r))},$$

where $W(r)$ is the conformational distribution function of ensemble, $V(r)$ is the potential energy of microscopic conformation r. The distribution can be thought as that of the canonical ensemble under effective potential $V_{eff}(r) = k_B T f(V(r))$ with the temperature T. Here k_B is the Boltzmann constant and we usually set it as unity in this paper. If $f(E) = \beta E = E/k_B T$, it is indeed the NVT canonical ensemble with the original potential

energy surface $V(r)$. It is easy to know the energy distribution in the $f(E)$ ensemble is

$$P(E) \propto \exp[S(E) - f(E)], \tag{2.1}$$

where $S(E) \equiv \ln g(E)$ and $g(E)$ is the density of states of system, which is defined as

$$g(E) \equiv \int \delta(E - V(r)) dr. \tag{2.2}$$

$S(E)$ is related to the micro-canonical entropy of system, which is an intrinsic property of the system itself and independent on the selection of ensemble function $f(E)$.

In this paper, we choose a particular $f(E)$ function,

$$f_{gce}(E) = \beta E + \frac{\alpha}{2}(E - U)^2 \tag{2.3}$$

with three parameters β, α and U, to present a special ensemble, named as generalized canonical ensemble (GCE). The usual NVT canonical ensemble is a special case of GCE with $\alpha = 0$. GCE can be thought as a derivative of the Gaussian ensemble presented by Hetheriongton et al. [12, 13] where $f(E) = \alpha(E - U)^2/2$. The GCE conformational distribution is

$$W_{gce}(\mu) = \exp[-f_{gce}(E_\mu)]. \tag{2.4}$$

Here microscopic conformations were re-denoted by the discrete index μ and the continuous potential energy surface $V(r)$ denoted by the discrete energy levels E_μ. As a matter of fact, GCE introduces the quadratic item into the weight exponent to generalize NVT ensemble. The parameters α and U are adjustable to make the width (and shape) of the energy distribution under control. Challa and Hetherington [13] had illustrated the relation between the energy distribution and α in the Potts model. We will further discuss how to use GCE generate a unimodal energy distribution even in phase-coexisting regions and how to combine with parallel tempering simulation.

We define the first order derivative of ensemble function

$$\tilde{\beta}(E) \equiv \frac{df_{gce}}{dE} \equiv \beta + \alpha(E - U). \tag{2.5}$$

Eq. (2.5) describes a straight line across the point (U, β) in the $E - \beta$ plane and the $\tilde{\beta}(E)$ curve of GCE generalizes the NVT horizontal line $\tilde{\beta}(E) = \beta$ by a slope α. In Fig. 1, we show the different $\tilde{\beta}(E)$ curves of NVT, GCE and the Ray's micro-canonical ensemble [14, 15].

Rewriting the energy distribution $P(E) = e^{Y(E)}$ in Eq. (2.1) for GCE, we get

$$Y(E) = S(E) - f_{gce}(E) + const. \tag{2.6}$$

We expand $Y(E)$ around a point $E = U_0$,

$$Y(E) = Y_0 + Y'(U_0)(E - U_0) + \frac{Y''(U_0)}{2}(E - U_0)^2 + o((E - U_0)^2). \tag{2.7}$$

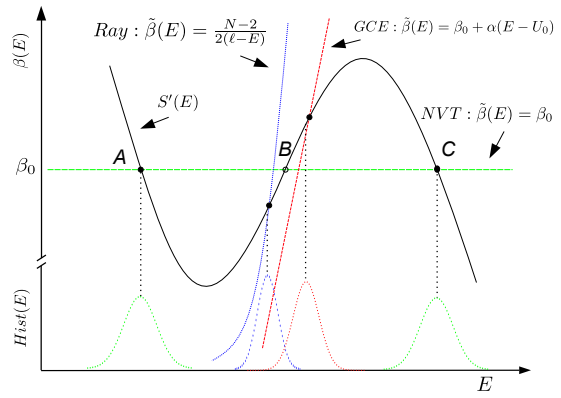

Figure 1: (Color online) Comparison of ensembles and their energy distributions in a first-order phase-transition system. The S-shaped curve $S'(E)$ is the derivative of the system entropic function. The canonical ensemble (NVT) curve of inverse temperature $\tilde{\beta}(E)$ crosses the S-shaped curve and exhibits two distribution-stable regions (A and C) and an unstable phase-coexistence region (around B). The generalized canonical ensemble (GCE) and Ray ensemble [14,15], unlike NVT, can visit the phase-coexistence region and yield single-peak distributions. The corresponding energy distributions under different ensembles are schematically plotted in the bottom panel.

Here $Y^{'}$ and $Y^{''}$ mean the first and second order derivative of $Y(E)$, respectively. In this paper, we will use the simple notations of derivatives. In Eq. (2.7), if selecting U_0 to make $Y^{'}(U_0)=0$ (i.e., the extremal point of $P(E)$), the condition of $P(E)$ following a Gaussian-like distribution is $Y^{''}(U_0)<0$, i.e., $\tilde{\beta}^{'}(U_0)>S^{''}(U_0)$, or specially $\alpha>S^{''}(U_0)$ in GCE. Then we have

$$P(E)\approx Ce^{-\frac{(E-\bar{U})^2}{2\sigma^2}},$$

where C is a constant. $\bar{U}$ and σ are the mean and variance of the Gaussian distribution, respectively. The mean of energy $\bar{U}$ approximately matches the position of the peak (the extremal point) of the Gaussian-like distribution, i.e., $\bar{U}\approx U_0$. It is worthy to point out, $S^{''}(E)$ is the intrinsic property of system, thus it is independent on the selection of simulation ensemble, $\tilde{\beta}^{'}(E)$. An energy region is stable (i.e., is sufficiently visited) in a special ensemble $\tilde{\beta}(E)$ when and only when the value of $S^{''}$ in the region is smaller than that of $\tilde{\beta}^{'}$. In NVT, since $\tilde{\beta}(E)\equiv 0$, we know that only the energy regions with negative $S^{''}$ is stable. The energy regions with positive $S^{''}$, which may correspond to multiple-phase coexistence, is unstable (i.e., could not be sufficiently visited). However, by selecting larger α in GCE to make $\alpha>S^{''}$, the phase-coexistence region can be stabilized. In other words, GCE can sufficiently visit the phase-coexistence regions and its energy distribution can be Gaussian-like. The energy mean and fluctuation in GCE approximately satisfy,

$$S^{'}(\bar{U})=\tilde{\beta}(\bar{U})=\beta+\alpha(\bar{U}-U), \tag{2.8a}$$

$$\frac{1}{\sigma^2}=\alpha-S^{''}(\bar{U}). \tag{2.8b}$$

Here the curve $\tilde{\beta}(\bar{U})$ characterizes the selected simulation ensemble, thus can be named as the exterior inverse temperature function. The curve $S^{'}(E)$ is determined by the system

itself, thus can be named as the interior inverse temperature function. More explicitly, the cross point of the curves $\tilde{\beta}(E)$ and $S^{'}(E)$ gives the mean energy $\bar{U}$ and the fluctuation of energy, σ^2, is dependent on the difference between the slopes of the two curves at the cross point. As α increases, the fluctuation σ decreases. By selecting suitable α in simulation, using the obtained energy mean and fluctuation, we can easily estimate the interior temperature at the mean energy, $S^{'}(\bar{U})$, thus form the whole curve $S^{'}(E)$ (or its integral, $S(E)$).

There may exist multiple cross points between the $\tilde{\beta}(E)$ and $S^{'}(E)$ curves. As shown in Fig. 1, for the 2-dimensional Potts model near the phase-coexisting region, the S-shaped $S^{'}(E)$ curve crosses with the NVT ensemble $\tilde{\beta}(E)=\beta_0$ curve at A, B and C points. According to the geometric relation between $\tilde{\beta}(E)$ and the $S^{'}(E)$ curve of the system [19, 20], we know that a cross point of the curves $\tilde{\beta}(E)$ and $S^{'}(E)$ is stable only when the slope of the former is larger than that of the latter, simulations only visit the neighboring energy regions of stable cross points and the energy distribution widths of simulations are determined by the differences of the two slopes at the stable cross points. Judging from the slopes of the curves $\tilde{\beta}(E)$ and $S^{'}(E)$, we could obtain Gaussian-like distributions around point B in the GCE and Ray's ensemble, but not in NVT ensemble, because around point B the slope of the interior temperature is positive. As a result, the system exhibits a first-order phase transition in NVT ensemble.

2.2 Parallel tempering on generalized ensembles

Similar to the conventional PT in canonical ensemble, PT simulation in generalized ensemble performs a group of M replicas at the same time, with the selected generalized ensemble distributions $W_i(\mu)$ in the $i=1,\cdots,M$ replicas. Each replica runs an independent Monte Carlo (MC) simulation and occasionally exchanges its own configurations with the neighboring replica based on the Metropolis criteria [21,22]. The calculation of physical quantity can be derived from these generated conformations after re-weighting. For example, to estimate the canonical average of any physical quantity Q, we can write the expression as

$$\langle Q\rangle=\frac{\sum_{i=1}^{M}\sum_{j}Q(\mu_{i,j})W_i(\mu_{i,j})^{-1}e^{-\beta E(\mu_{i,j})}}{\sum_{i=1}^{M}\sum_{j}W_i(\mu_{i,j})^{-1}e^{-\beta E(\mu_{i,j})}}, \tag{2.9}$$

where $\mu_{i,j}$ is the j^{th} conformation in the i^{th} replica.

Assuming that replica 1 stays in state μ_1 and replica 2 in state μ_2, they take the probability distributions $P_1(\mu_1)\propto e^{-f_1(E_{\mu_1})}$ and $P_2(\mu_2)\propto e^{-f_2(E_{\mu_2})}$, respectively. The joint probability density of the entire system takes the value $P_1(\mu_1)P_2(\mu_2)$ and $P_1(\mu_2)P_2(\mu_1)$ before and after the exchange, respectively. According to the detailed balance condition, we

have the Metropolis acceptance probability of the configuration exchange,

$$\alpha[(\mu_1,\mu_2)\to(\mu_2,\mu_1)]=\min\Big\{1,\frac{P_1(\mu_2)P_2(\mu_1)}{P_1(\mu_1)P_2(\mu_2)}\Big\}=\min\big\{1,\exp(\triangle A)\big\}, \tag{2.10}$$

where

$$\Delta A=-f_1(E_2)-f_2(E_1)+f_1(E_1)+f_2(E_2)=\int_{E_1}^{E_2}[\tilde{\beta}_2(E)-\tilde{\beta}_1(E)]dE, \tag{2.11}$$

i.e., the area of the curves enclosed by $\tilde{\beta}_2(E)$ and $\tilde{\beta}_1(E)$ in the energy range E_1 and E_2. Here $\tilde{\beta}_i(E)=df_i(E)/dE$ and $E_i=E_{\mu_i}$ for $i=1,2$. The result is correct in any ensemble (i.e., any $\tilde{\beta}(E)$). In NVT ensemble, it recovers the well known result, $\Delta A=\Delta\beta\Delta E$, where $\Delta\beta=\beta_2-\beta_1$ and $\Delta E=E_2-E_1$. In GCE, if

$$\begin{cases}\tilde{\beta}_1(E)=\beta_1+\alpha_1(E-U_1),\\ \tilde{\beta}_2(E)=\beta_2+\alpha_2(E-U_2),\end{cases} \tag{2.12}$$

we have

$$\Delta A=\Big[\Delta\beta+\frac{\Delta\alpha}{2}\Delta E-(U_2\alpha_2-U_1\alpha_1)\Big]\Delta E, \tag{2.13}$$

where $\Delta\alpha=\alpha_2-\alpha_1$.

We investigate $\tilde{\beta}_1(E)$ and $\tilde{\beta}_2(E)$ in a system with first-order phase transition, as shown in Fig. 2. In the single-phase region, the conformations of adjacent replicas can overlap each other, Eq. (1.1) can be applied to estimate SAR. For example, the SAR between the states A and B of two NVT ensembles is determined by

$$\kappa\equiv(E_B-E_A)/(\sigma_B+\sigma_A).$$

If $\kappa\sim\mathcal{O}(1)$, from Eq. (1.1), SAR is also $\mathcal{O}(1)$, thus PT simulation is sufficient. If $\kappa\gg1$, SAR will be almost zero, thus PT simulation is insufficient, unless more intermediate replicas are applied. As N increases, κ increase as $\mathcal{O}(N^{1/2})$, it means that $\mathcal{O}(N^{1/2})$ intermediate replicas must be inserted between NVT_1 and NVT_2 to make SAR between adjacent replicas be of $\mathcal{O}(1)$.

In multiple-phase coexistence regions, for example in $[E_A,E_D]$, however, no matter how many intermediate NVT ensembles are applied, the middle part of the energy range (the canonical unstable phase-coexisting region) could not be frequently visited by any of these replicas, κ is always much larger than unity. In these case, the acceptance rate of exchanges between different phases, such as the states A and D, will be determined by the area δS_{AHDJ} rather than κ. Since the energy difference of two phases is in $\mathcal{O}(N)$, we have to set $\delta\beta\sim\mathcal{O}(1/N)$ in order to make the area $\Delta S_{AHDJ}\sim\mathcal{O}(1)$, (thus the inter-phase SAR, $\exp[-\delta S]$, is also in $\mathcal{O}(1)$). Here $\delta\beta$ is the difference of β between adjacent NVT ensembles. It is worthy to point out that the inter-phase exchange is more important in reaching equilibrium among phases than the intra-phase exchange. The average value of SAR in

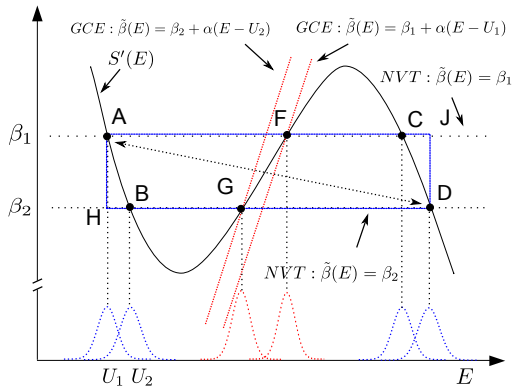

Figure 2: (Color online) Comparisons of the Swap Acceptance Rate (SAR) of parallel tempering in the ensembles NVT and GCE. The derivative of system entropic function $S'(E)$ indicates the system of first-order phase transition. In NVT simulations, the SAR of replica exchanging in the same phase (e.g., from A to B) is calculated from two overlapping unimodal distributions, whereas the SAR value in the different phases, for example state exchanging from A to D, is determined approximately by the area δS_{AHDJ}. In GCE simulations, unimodal energy distributions can be produced to keep SAR steady even in phase-coexisting region.

whole simulation, which contributes from both intra-phase and inter-phase exchanges, actually could not well characterize the efficiency of PT in enhanced sampling. For example, if we select $\delta\beta$ based on Eq. (1.1) so that $\kappa_{AB}\sim 1$ but $\delta S_{AHDJ}\gg 1$, i.e., the intra-phase swaps are accepted with a larger probability but the inter-phase swaps are nearly unable to be accepted. The value of SAR may fluctuate between a large value (corresponding to intra-phase exchanges) and almost zero (corresponding to inter-phase exchanges). In these cases, the large SAR does not indicate the PT simulation is sufficient. Therefore, a significant SAR in the short trial NVT-PT simulation might become very small in the next segments of simulation. It means the traditional way to set temperatures of replicas of PT could not be used. Actually, in setting parameters of replicas in phase-coexisting regions, instead of requiring $\kappa\sim 1$, we should require that the area enclosed by adjacent $\tilde{\beta}$ curves and the corresponding average energies in two phases, such as δS_{AHDJ}, is of $\mathcal{O}(1)$. Thus, if supposing the β range of phase-coexisting region is independent on the system size N (or decreasing not faster than $N^{-1/2}$ as increasing N), the number of required replicas in phase-coexisting regions will increase faster than the previous expectation $\mathcal{O}(N^{1/2})$.

In GCE-PT, we can apply a positive α and adjust U to form a stable unimodal energy distribution even in the phase-coexisting regions of system, where $S''(E)$ is positive so that it is unstable in NVT ensemble. Therefore, by inserting intermediate GCE replicas, the entire energy range can be completely covered, i.e., all κ can always be set of $\mathcal{O}(1)$ and SAR nearly remains a constant during the simulation. By selecting suitable α, it is easy to make the energy fluctuation of GCE be also $\mathcal{O}(N^{1/2})$ but the single-peak energy distribution is kept, thus the previous conclusions of NVT-PT in single-phase regions are correct in both single-phase and multiple-phase regions for GCE-PT. For example, the parameters of GCE-PT replicas can be easily set from short trial simulations, Eq. (1.1) and

SAR characterizes the efficiency of PT in enhanced sampling and the number of require replicas is in $\mathcal{O}(N^{1/2})$ in the entire energy range.

3 Results of 2D Potts model

We take the well known 2D Potts model as an example to demonstrate the advantages of GCE-PT. The Hamiltonian of 2D Potts model is defined as

$$H=-\sum_{\langle i,j\rangle} J\delta(q_i,q_j),$$

where the summation is taken over all nearest neighboring pairs on 2D lattice, each spin takes the value $q_i=1,\cdots,Q$ and δ is the Kronecker delta. For the 2D Potts model, when $Q>4$, it exhibits the first order phase transition, with the transition temperature $\beta_c=1/(K_BT_c)=\ln(1+\sqrt{Q})$ in the thermodynamical limit [23, 24]. For convenience, in the following studies, we set $J=1$ and $Q=10$ and take periodic boundary condition in the 2D lattice.

3.1 Fluctuation of SAR

We used $N=L^2$, $L=32$, $Q=10$ Potts model to test the fluctuation of SAR along time in phase-coexistence region.

In NVT-PT simulation, the inverse temperatures of three replicas uniformly take

$$[\beta_1,\,\beta_2,\,\beta_3]\,=[1.4195,\,1.4230,\,1.4265],$$

where the phase transition point in the thermodynamical limit $\beta_c=1/T_c\approx 1.42606$ is between β_2 and β_3. Replica exchange strategy takes the even/odd algorithm [25], that is, each replica exchanges its conformation with its two neighbors. The entire run of each replica is 10^6MC cycles (1MC cycle $=N$ random spin-varying steps) and sampling once each MC cycle. The entire simulation is equally divided into 20 segments (i.e., each segment is $10^6/20$MC cycles), in each segment we independently calculate the average SAR, s_t, $t=1,\cdots,20$.

Similarly, we performed three GCE-PT replicas, whose conformations can continuously cover the coexistence region. For convenience, we rewrite the GCE weight exponent $f_i(E)$ as

$$f_i(E)=\beta_iE+\frac{\alpha_i}{2N}(E-u_iN)^2=N\Big[\beta_ie+\frac{\alpha_i}{2}(e-u_i)^2\Big], \tag{3.1}$$

where $e=E/N$, $\beta_i=1.426$, $\alpha_i=1.2$ $(i=1,2,3)$ and the three u_i also take the uniformly spaced values as follows

$$[u_1,\,u_2,\,u_3]=[-1.41,\,-1.44,\,-1.47].$$

The SAR in GCE-PT was calculated in the same way as NVT-PT.

We check the conformational energy distribution (Fig. 3) and investigate the SAR values changing over the simulation time t (Fig. 4). In NVT-PT, each of the three NVT distributions shows a double-peak distribution characterized by the first order phase transition and the SARs between them fluctuate largely as time t. When two adjacent replicas stay in the same phase, their energy distributions largely overlap and the SAR value is large. Whereas in different phases, since the energy difference of the two phases is much larger than the summation of energy fluctuations in the phases (i.e., $\kappa \gg 1$), the acceptance rate of inter-phase exchanges is determined by the area $\delta S = \delta\beta\delta E$. In the simulation, $\delta\beta = 0.0035$, the energy difference between two phases is about $600 \sim 800$ (see Fig. 3), thus $\delta S \approx 2 \sim 3$, the acceptance rate, $e^{-\delta S}$, is small but still significant. It implies that the applied temperature interval is slightly large but still suitable for getting sufficient exchanges between different phases. In GCE-PT, each of the three GCE histograms displays a single peak in the phase-coexisting region and the SAR between them is nearly a constant in time, about 0.45. Thus, the parameters of replicas can be easily set from short trial simulations. In addition, GCE-PT can sufficiently visit phase-coexisting regions then can detect multiple-phase coexistence.

3.2 Efficiency of sampling

Taking $L = 60$ and $Q = 10$ Potts model as an example, we compare the efficiencies of NVT-PT and GCE-PT simulations. Wang-Landau method [26] was also performed for comparison.

In NVT-PT, we simulated 40 replicas, each of them take β_i from an evenly spaced interval $[1.401, 1.45]$, thus $\delta\beta \approx 0.001$. Since the energy difference between two phases in the system is about 3000, the area between two phases enclosed by $\tilde{\beta}(E)$ curves of adjacent replicas, $\delta S \approx 3$, is slightly large but still of $\mathcal{O}(1)$. It implies the acceptance rate of inter-phase exchanges is small but may be still significant. Similarly, the GCE-PT simulation contains 40 replicas, each of them take u_i from an evenly spaced interval $[-1.785, -0.853]$ and other parameters of GCE take the same values: $\alpha_i = 1.5$ and $\beta_i = 1.426$, $i = 1, \cdots, 40$ (see Eq. (3.1)). It is possible to use smaller (and energy-dependent) α to make GCE distribution be still single-peak, then the number of replicas could be further decreased. The suitable α can be selected by estimating the values of $S''(E)$ at different E points from trial simulations. In this paper, we do not focus on selection of α in GCE-PT in order to decrease the number of replicas, but show the ability of GCE-PT in covering phase-coexisting regions. In both NVT-PT and GCE-PT simulations, each replica runs 10^6MC cycles, which is divided into 20 equal segments and we estimate SAR in each segment, s_t $(t = 1, \cdots, 20)$, in the same way as the previous sections. In Wang-Landau method, we use the terminated factor $f = 7 \times 10^{-9}$ and 85% of the flatness (these parameters are explained in [27]).

In Fig. 5(a) and (b), we show the energy histogram of NVT-PT and GCE-PT simulations, respectively. The results clearly show the single-peak distribution of GCE even in

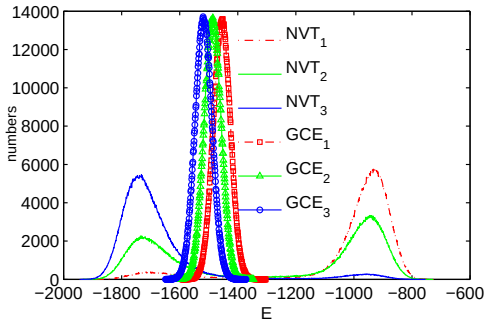

Figure 3: (Color online) The energy distributions (histogram) of the parallel tempering simulations of 2D $Q=10$ Potts Model $(N=32\times32)$ on NVT and GCE, respectively.

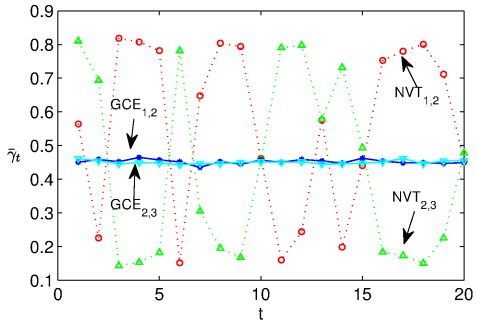

Figure 4: Comparisons of SAR in time t: $\bar{\gamma}_t$ between replicas of NVT (and GCE) parallel tempering simulations. $\text{NVT}_{i,j}$ denotes $\bar{\gamma}_t$ between $\text{NVT}_i \longleftrightarrow \text{NVT}_j$ and $\text{GCE}_{i,j}$ denotes $\text{GCE}_i \longleftrightarrow \text{GCE}_j$. $\bar{\gamma}_t$ is calculated every $10^6/20$MC cycles.

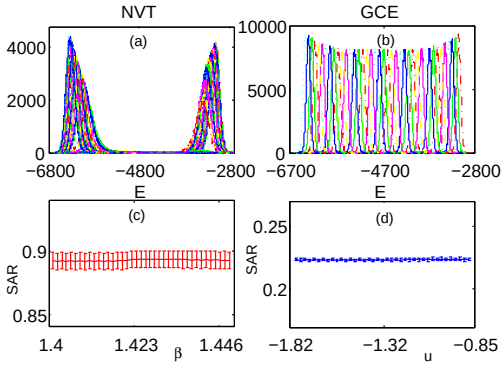

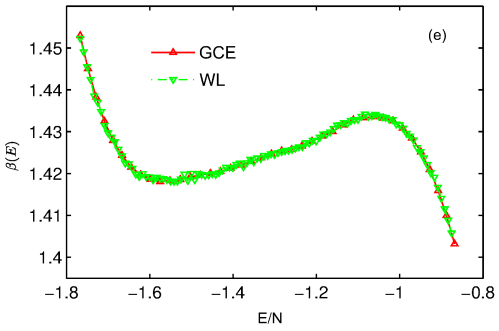

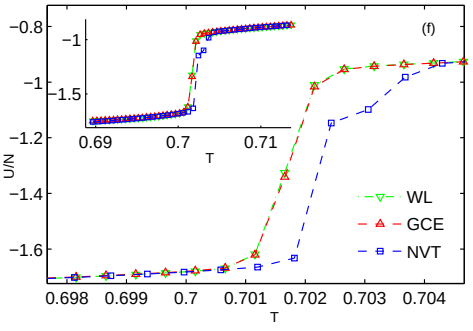

Figure 5: (Color online) Using GCE-PT, NVT-PT and Wang-Landau method to estimate physical quantities. (a) and (b) are the energy histogram of the 40 replicas of NVT-PT and GCE-PT. (c) and (d) are the 39 SAR values with error bars of NVT-PT and GCE-PT. The interior inverse temperature functions (the derivative of logarithmic density of states) calculated from Wang-Landau method (e, WL) and GCE-PT (e, GCE). GCE-PT, NVT-PT and Wang-Landau method are applied to estimate the internal energy function of temperature T (f). The inset gives the U/N functions of T in larger temperature range.

the phase-coexisting region and the overlapping between adjacent GCEs's distributions. Thus their SAR can be expected from Eq. (1.1) and the number of replicas is of $\mathcal{O}(N^{1/2})$. In contrast, the energy distributions in NVT ensembles are double-peaked in the phase-coexisting regions, the energy gap between two phases is proportional to N, thus in the gap (i.e., phase-coexisting) region, the β interval of adjacent replicas must decreases as

$\mathcal{O}(1/N)$, more NVT replicas than $\mathcal{O}(N^{1/2})$ might be needed in the phase-coexistence region. In Fig. 5(c) and (d), we show the means and fluctuations of SARs in NVT-PT and GCE-PT, respectively. SARs in NVT-PT have larger mean values and larger fluctuations in comparison with that in GCE-PT.

In Fig. 5(e), we estimate the density of states (more exactly, the interior inverse temperature $S^{'}(E)$) of 2D Potts model by GCE-PT and Wang-Landau method. The two results are consistent with each other. In principle, it is also possible to estimate $S^{'}(E)$ of the coexistence region from NVT-PT,

$$S^{'}(E)=\beta_i+\frac{H_i^{'}(E)}{H_i(E)} \tag{3.2}$$

for any NVT$_i$ with the inverse temperature β_i. $H_i(E)$ is the histogram of the i^{th} NVT replica. However, in practice, the estimate of $S^{'}(E)$ requires sufficient $H(E)$, thus the $S^{'}(E)$ in the phase-coexisting regions can not be well estimated in NVT-PT, since no replica visit the region frequently.

In Fig. 5(f), we present the $U-T$ diagrams based on the estimation of GCE-PT and Wang-Landau method. In the coexistence region, the average energy estimated by NVT-PT deviates from the other two results; in single-phase regions, the results of all the three methods are consistent each other. Note that in Fig. 5(c) the average SAR of NVT-PT (about 89%) turns out much higher than GCE-PT's 22%. However, the high SAR in NVT-PT does not mean efficient sampling. The main reason is that most of the conformational exchanges in NVT-PT are intra-phase exchanges and the inter-phase exchanges are still not sufficient, thus the equilibrium between phases is hard to be reached.

4 Conclusions and discussions

Parallel tempering on NVT ensemble (NVT-PT) is an important enhanced sampling simulation method, which is widely used in many different systems. Swap acceptance rate (SAR) between adjacent replicas is required to be significant for efficiently sampling and the requirement is applied to set parameters of replicas. The SAR is usually estimated based on the ratio of the energy difference of adjacent replicas to the summation of their fluctuations, $\kappa=(\bar{E}_2-\bar{E}_1)/(\sigma_1+\sigma_2)$, thus the number of required replicas in NVT-PT is expected to be in $\mathcal{O}(N^{1/2})$ as the size of system N. However, all these well known results about NVT-PT may be incorrect in phase-coexisting regions where we usually hope to use parallel tempering simulations. In the phase-coexisting regions, SAR of NVT-PT may be not steady in time thus it is difficult to set parameters of replicas by short trial simulations. In addition, the number of required replicas in the phase-coexisting regions might be of $\mathcal{O}(N)$ rather than the usual expectation in single-phase regions, $\mathcal{O}(N^{1/2})$.

In this work, we find that parallel tempering on generalized canonical ensemble (GCE-PT) is able to obtain the steady and efficient SAR even in the phase-coexisting regions, since GCE can regulate the energy distribution to avoid the occurrence of the first

order phase transition. GCE can visit both the phase-coexisting and single-phase regions with Gaussian-type energy distribution and the energy fluctuation could be of $\mathcal{O}(N^{1/2})$ in the whole energy region, thus the previous results about NVT-PT in single-phase regions can still hold for GCE-PT in both single-phase and phase-coexisting regions. For example, due to the steady SARs in GCE-PT, we can easily determine the optimal parameters in parallel tempering; GCE-PT only needs $\mathcal{O}(N^{1/2})$ replicas in both single-phase and coexisting regions; SARs can be well used to evaluate the efficiency of GCE-PT in enhanced sampling. Since the energy fluctuation in GCE with positive α is slightly smaller than that in NVT, in single-phase regions, the number of replicas in GCE-PT might be slightly larger than that in NVT-PT. However, in phase-coexisting regions, less replicas in the GCE-PT are needed. In practical simulations, we may apply different α in different replicas to get both the Gaussian-type distribution and larger energy widths. For example, first we can apply $\alpha = 0$ (i.e., NVT ensemble) to run a trial PT simulation, then increase α in some replicas but keep $\alpha = 0$ in the others. In one word, as a generalization of NVT-PT, the new method, GCE-PT, is more efficient and more flexible in enhanced sampling of complex systems.

Acknowledgments

X. Zhou acknowledges Chinese Academy of Sciences for the support of the "hundreds talents" program at Graduate University of Chinese Academy of Sciences (GUCAS). He also thanks the Max Planck Society (MPG), the Korea Ministry of Education, Science and Technology (MEST), for the support of the Independent Junior Research Group at the Asia Pacific Center for Theoretical Physics (APCTP), Korea. He recently left APCTP to join GUCAS and part of the work was done before his movement. Z.-C. Ou-Yang thanks the support of National Basic Research Program of China (973 Program) No. 2007CB935903. We also thanks the helpful discussions with Prof. Ming Li of GUCAS.

References

[1] Robert H. Swendsen and Jian-Sheng Wang, Replica monte carlo simulation of Spin-Glasses, Phys. Rev. Lett., 57(21) (1986), 2607.
[2] Koji Hukushima and Koji Nemoto, Exchange monte carlo method and application to spin glass simulations, J. Phys. Soc. Japan, 65(6) (1996), 1604–1608.
[3] David J. Earl and Michael W. Deem, Parallel tempering: theory, applications and new perspectives, Phys. Chem. Chem. Phys., 7(23) (2005), 3910.
[4] Robert Denschlag, Martin Lingenheil and Paul Tavan, Optimal temperature ladders in replica exchange simulations, Chem. Phys. Lett., 473(1-3) (2009), 193–195.
[5] K. Y. Sanbonmatsu and A. E. García, Structure of met-enkephalin in explicit aqueous solution using replica exchange molecular dynamics, Proteins, 46(2) (2002), 225–234, PMID: 11807951.

[6] Alexandra Patriksson and David van der Spoel, A temperature predictor for parallel tempering simulations, Phys. Chem. Chem. Phys., 10(15) (2008), 2073.
[7] David A. Kofke, On the acceptance probability of replica-exchange monte carlo trials, J. Chem. Phys., 117(15) (2002), 6911.
[8] Nitin Rathore, Manan Chopra and Juan J. de Pablo, Optimal allocation of replicas in parallel tempering simulations, J. Chem. Phys., 122(2) (2005), 024111.
[9] Aminata Kone and David A. Kofke, Selection of temperature intervals for parallel-tempering simulations, J. Chem. Phys., 122(20) (2005), 206101.
[10] Walter Nadler and Ulrich Hansmann, Generalized ensemble and tempering simulations: a unified view, Phys. Rev. E, 75(2) (2007), 026109.
[11] T. Neuhaus and J. Hager, Free-energy calculations with multiple gaussian modified ensembles, Phys. Rev. E, 74(3) (2006), 036702.
[12] Murty S. S. Challa and J. H. Hetherington, Gaussian ensemble: an alternate monte carlo scheme, Phys. Rev. A, 38(12) (1988), 6324–6337.
[13] Murty S. S. Challa and J. H. Hetherington, Gaussian ensemble as an interpolating ensemble, Phys. Rev. Lett., 60(2) (1988), 77–80.
[14] John R. Ray, Microcanonical ensemble monte carlo method, Phys. Rev. A, 44(6) (1991), 4061–4064.
[15] V. Martin-Mayor, Microcanonical approach to the simulation of first-order phase transitions, Phys. Rev. Lett., 98(13) (2007), 137207.
[16] Marius Costeniuc, Richard S. Ellis, Hugo Touchette and Bruce Turkington, The generalized canonical ensemble and its universal equivalence with the microcanonical ensemble, J. Stat. Phys., 119(5) (2005), 1283–1329.
[17] M. Costeniuc, R. S. Ellis, H. Touchette and B. Turkington, Generalized canonical ensembles and ensemble equivalence, Phys. Rev. E, 73(2) (2006), 026105.
[18] H. Touchette, M. Costeniuc, R. S. Ellis and B. Turkington, Metastability within the generalized canonical ensemble, Phys. A, 365(1) (2006), 132–137.
[19] L. Velazquez and S. Curilef, Geometrical aspects and connections of the energy-temperature fluctuation relation, J. Phys. A Math. Theor., 42(33) (2009), 335003.
[20] L. Velazquez and S. Curilef, A thermodynamic fluctuation relation for temperature and energy, J. Phys. A Math. Theor., 42 (2009), 095006.
[21] Jaegil Kim and John E. Straub, Optimal replica exchange method combined with tsallis weight sampling, J. Chem. Phys., 130(14) (2009), 144114.
[22] Jaegil Kim, Thomas Keyes and John E. Straub, Generalized replica exchange method, J. Chem. Phys., 132(22) (2010), 224107.
[23] J. H. Hetherington and Daniel R. Stump, Sampling a gaussian energy distribution to study the phase transitions of the $z(2)$ and $u(1)$ lattice gauge theories, Phys. Rev. D, 35(6) (1987), 1972–1978.
[24] F. Y. Wu, The potts model, Rev. Mod. Phys., 54(1) (1982), 235–268.
[25] Martin Lingenheil, Robert Denschlag, Gerald Mathias and Paul Tavan, Efficiency of exchange schemes in replica exchange, Chem. Phys. Lett., 478(1-3) (2009), 80–84.
[26] F. Wang and D. P. Landau, Efficient, multiple-range random walk algorithm to calculate the density of states, Phys. Rev. Lett., 86(10) (2001), 2050–2053.
[27] Fugao Wang and D. Landau, Determining the density of states for classical statistical models: a random walk algorithm to produce a flat histogram, Phys. Rev. E, 64(5) (2001), 056101.